International Journal of Bridge Engineering (IJBE), Vol. 6, No. 2, (2018), pp. 85-107

SIMPLIFIED COMPUTATION OF TIME DEPENDENT EFFECTS OF SEGMENTAL BRIDGES

Atef Gendy[1] and Magdy Rashed[2]

[1,2] Cairo University, Structural Engineering Dept., Egypt
e-mail: agendy@hotmail.com, mrr.mikhail@yahoo.com

ABSTRACT: Step-by-step solution strategy for segmental prestressed concrete bridge calls for: (i) time dependent effects of creep and shrinkage of concrete, and relaxation of prestressed steel; (ii) losses due to friction and anchor setting of prestressing tendons; (iii) sequence of construction, and change of geometry and support conditions; (iv) tension stiffening effect of concrete after cracking; (v) effects of nonprestressed steel on the redistribution of stresses. These significant parameters have been accounted for to obtain the time dependent serviceability analysis of several segmental prestressed concrete bridges over the Nile River utilizing Eurocode specifications. Redistribution of stresses in concrete, prestressed as well as nonprestressed steels due to time-dependent effects during construction and after a long time of operation is one of our objectives. Such redistribution of stresses/moments produced by time dependent analysis is to be place in an intermediate state between the analyses obtained from two different cases: (a) adding all partial stresses for each construction step using corresponding statical system; (b) assuming all loads and prestress forces to be applied on the final statical system. This paper is to report on estimated contributions of each of the two time-independent cases in order to minimize the difference with results obtained from the time-dependent analysis. To this end, a number of robust, and computationally efficient, algorithms are presented and integrated through software ESTMATOR, which casts the optimum parameters as a minimum-error nonlinear optimization problem with constraints and solves it with the sequential quadratic nonlinear programming technique.

KEYWORDS: Segmental bridge**,** prestressed concrete, time dependent effects, sequence of construction, parameter estimation, optimization technique**.**

1 INTRODUCTION

Significant progress has been made over the years in the development of step-by-step methodologies to account for the time dependent effects in the analysis of segmental prestressed concrete bridges. Article on design, analysis, and construction of segmental bridges have been published by many researches and comparisons are made between the analytical results and the measured responses of actual structures [e.g., 1, 2]. Attention is also given on the deformations and internal moment redistribution due to creep and shrinkage of concrete when the structural system is changed during construction [3-5]. In particular, Bishara and Papakonstantinou [3] investigated the time dependent deformation of cantilever construction bridges before and after closure. Cruz et al. [6] introduced a nonlinear analysis method to calculate the ultimate strength of bridges.

The development of sophisticated computer programs for time dependent analysis of segmental bridges is a tedious task. In addition to their limitations in wide use, because of the complexity of the practical applications, such programs require engineers with special skills. Consequently, a simple formula for estimating the internal moment redistribution due to creep and shrinkage of concrete, which can be appropriate for use by design engineers, has been continuously required. Trost and Wolff [5] introduced a simple formula which can simulate internal moment redistribution with a superposition of the elastic moments from each construction step. A similar approach has been presented by the Prestressed Concrete Institute and Post-Tensioning Institute [7]. A simple equation has been introduced in [8] to calculate the internal moment redistribution in segmental bridges after completion of construction. All these simplified formulae are developed on the basis of the combination of the summation the elastic moments occurred at each construction step, $\sum M_o$, and the moment obtained by assuming that the entire structure is constructed in one step, M_c as

$$M_T = \sum M_o + (M_c - \sum M_o)\ \Re \tag{1}$$

where $\Re$,which may take different forms, is basically a function accounting for concrete aging, and creep behavior. Equation (1) can be rewritten in the different form as

$$M_T = (1-\Re)\sum M_o + \ \Re\ M_c \tag{2}$$

In this research, such form shown in Eq. (2) has been adapted to obtained moment redistribution due to dead load and prestressed considering the time dependent effects through optimization technique. Knowing that the long term moment is a combination of the two cases: (a) summation of moments due to own weight and prestressing during bridge construction obtained from different statical system; (b) moment obtained as if the bridge is constructed in one step, the contribution of each of the two cases can be obtained by minimizing the difference between the results from the time dependent analysis and those provided by certain contribution from the two time-independent cases.

The primary objective of this research is to develop a computationally efficient methodology to identify the estimated parameters needed to simulate the redistribution of the stresses/moments obtained by the time dependent analysis from the conventional time independent analyses performed for the class of segmental prestressed bridges. To this end, an integrated software program called ESTMATOR has been developed. Its overall strategy is outlined as follows: (a) primal analysis tools; and (b) optimization technique of an error/cost function with sensitivity analysis. With regard to item (a), we adopted step-by-step solution strategy for segmental prestressed concrete bridge which includes time dependent effects due to creep and shrinkage of concrete and relaxation of prestress steel, losses due to friction and anchor setting of prestressed tendons; sequence of construction and change of geometry and support conditions (if any); tension stiffening effect of concrete after cracking; and effects of nonprestressed steel on the redistribution of stresses. The previously developed, step by step analysis, strategy [9] has been adopted here for shrinkage and creep of concrete utilizing Eurocode [10] and CEB-FIP Model Code [11]. In connection with item (b), the optimization module is used to cast the estimation of the parameters as a minimum-error, objective, nonlinear optimization problem, which is subsequently solved using the sequential quadratic programming technique [12-16]. Such optimization technique is based on an iterative formulation and solution of several quadratic-programming sub-problems. Each sub-problem may be obtained utilizing a quadratic approximation of the system Lagrangian and a linearization of the constraints at each iteration. At present, this is known to be one of the best available, gradient-based, nonlinear optimization techniques. Several features have also been incorporated into ESTMATOR to facilitate the estimation of the analysis parameters. These include the following: (i) design variable formulation which includes variable grouping, i.e., active/passive variables, (ii) constraint formulation including variable bounds, (iii) general scaling of variables as well as objective function; and (iv) the use of quasi-Newton and line search techniques for solution enhancements. In brief, the estimator tool is of the optimal strategy type, in which the nonlinear mathematical programming problem is solved utilizing a successive quadratic programming technique. The overall program has been designed to be robust, reliable, easy-to-operate, and portable.

An outline of the remainder of the paper is as follows. In section 2, the evolution of material properties such as elastic modulus, creep, shrinkage, and relaxation has been briefly described according to design specifications Eurocode [10]. In section 3, the general step-by-step scheme accounting for the time-dependent effects in segmental prestressed concrete bridges is presented. Details of the stress update algorithm for instant as well as time-dependent effects are also given. A brief description of the optimization technique developed is discussed in section 4. Numerical results and simulations are presented in section 5. These include time dependent serviceability analysis of two segmental pre-stressed concrete bridges over the Nile River. Redistribution of stresses/moments in concrete, pre-stressed as well as non-prestressed steels due to time-dependent effects during construction and after a long time of operation is investigated. The optimization methodology developed has been utilized to identify the estimated parameters needed to simulate the redistribution of the stresses/moments obtained by the time dependent analysis from the conventional time independent analyses performed for the class of segmental prestressed bridges. Finally, a summary and conclusions are given in section 6.

2 EVOLUTION OF MATERIAL PROPERTIES

The evolution of material properties such as elastic modulus, creep, shrinkage, and relaxation has been briefly described according to design specifications and Eurocode [10].

Starting with the elastic modulus of concrete, it can be calculate based on the compressive strength according to

$$E_c = \alpha_E \left(\frac{f_{cm}}{f_{cmo}} \right)^{1/3} \tag{3}$$

where E_c is the modulus of elasticity of concrete at an age of 28 days (MPa), α_E $=2.15(10)^4$ (MPa), f_{cm} the compressive strength of concrete at an age of 28 days (MPa), and f_{cmo} = 10 (MPa). When an elastic analysis is performed, a lower value of the modulus of elasticity should be used to consider the initial plastic cracking due to plastic shrinkage. It is suggested that this is done by decreasing the elastic modulus according to E_{cs}=0.85E_c, where E_{cs} is the secant modulus in the elastic range of concrete. To take into account the age of concrete, the time dependent function may be used

$$E_c(t) = \sqrt{\exp^{s\left(1-\sqrt{\frac{28}{t}}\right)}}\; E_{cs} \tag{4}$$

where t is the age of concrete in days and s is a coefficient depending on the cement type and is equal to 0.20 for rapidly hardening cement for high strength concrete, 0.25 for normal and rapidly hardening cement and 0.38 for slowly hardening cement. The creep coefficient can be calculated as

$$\varphi(t,t_o) = \varphi_o \; \beta_c(t - t_o) \tag{5}$$

Where φ_o is the notional creep coefficient, and $\beta_c(t\text{-}t_o)$ is the time function describing the developing of creep with time. The notional creep coefficient can be estimated as

$$\varphi_o = 1 + \frac{1 - RH/100}{0.46(h_o/100)^{1/3}} \; \frac{5.3}{\sqrt{f_{cm}/10}} \; \frac{1}{0.1 + \sqrt{t_o}} \tag{6}$$

and the time-development function is expressed as

$$\beta_c(t-t_o)=\left(\frac{t-t_o}{\beta_H+t-t_o}\right)^{0.3} \tag{7}$$

with

$$\beta_H=150\left(1+\left(1.2\frac{RH}{100}\right)^{18}\right)\frac{h_o}{100}+250 \quad \leq \; 1500 \tag{8}$$

In the above, *RH* is the relative humidity of the ambient environment in percent; t is the age of concrete is days at the moment considered, t_o is the age of concrete at loading in days; h_o is the notional size of the member in mm which is equal to $2A_c/u$, where A_c is the cross section area, and u is the perimeter of the member in contact with atmosphere.

The total shrinkage strain, ε_{cs}, is composed of two components, the drying shrinkage strain, ε_{cd}, and the autogenous shrinkage strain, ε_{ca}. The drying shrinkage strain develops slowly, since it is a function of the migration of the water through the hardened concrete. The autogenous shrinkage strain develops during hardening of the concrete: the major part therefore develops in the early days after casting. Autogenous shrinkage is a linear function of the concrete strength. It should be considered specifically when new concrete is cast against hardened concrete. The drying shrinkage strain ε_{cd} may be calculated from

$$\varepsilon_{cd}=\frac{t-t_s}{(t-t_s)+0.04\sqrt{t^3}}\;k_h\;\varepsilon_{cd,\infty} \tag{9}$$

where k_h is a coefficient depending on the notional size h_0, which has a value 1.0 to 0.70 for h_o equal to 100 to 500, respectively; t is the age of the concrete at the moment considered in days; t_s is the age of the concrete (days) at the beginning of drying shrinkage (normally this is at the end of curing). The basic drying shrinkage, $\varepsilon_{cd,\infty}$;can be expressed as

$$\varepsilon_{cd,\infty}=\left[(220+110\,\alpha_{ds1})\,.\;\exp\left(-\alpha_{ds2}\,.\frac{f_{cm}}{f_{cmo}}\right)\right]\,.\,10^{-6}\,.\,\beta_{RH} \tag{10}$$

with

$$\beta_{RH}=-1.55\left[1-\left(\frac{RH}{100}\right)^3\right] \qquad for \quad RH \prec 99\%\left(\frac{3.5\,f_{cmo}}{f_{cm}}\right)^{0.1} \tag{11a}$$

$$\beta_{RH}=0.25 \qquad for \quad RH \geq 99\%\left(\frac{3.5\,f_{cmo}}{f_{cm}}\right)^{0.1} \tag{11b}$$

where a_{ds1} and a_{ds2} are coefficients depending on the cement type and are equal to 6 and 0.11, respectively for rapidly hardening high strength cement; 4 and

0.12, respectively for normal and rapidly hardening cement; and 3 and 0.13, respectively for slowly hardening cement.
The autogenous shrinkage strain can be expressed as

$$\varepsilon_{ca} = \left(1 - \exp^{\left(-0.2\,\sqrt{t}\right)}\right) \varepsilon_{ca}(\infty) \qquad (12)$$

where:

$$\varepsilon_{ca}(\infty) = 2.5\,(f_{ck} - 10)\,10^{-6} \qquad (13)$$

where f_{ck} is the characteristic compression strength of concrete.
The intrinsic relaxation suggested by Ghali and Trevino [17] based on experimental values given in the CEB-FIP Model Code [11] and the FIP report on prestressing steel [18] has been adopted here. The expression for such intrinsic relaxation can be written as

$$\Delta\sigma_{pr}(t, t_o) = -k\,\eta_t\,\sigma_{pso}\left(\frac{\sigma_{pso}}{f_{pu}} - 0.4\right)^2 \quad , \quad \frac{\sigma_{pso}}{f_{pu}} \succ 0.4 \qquad (14)$$

where σ_{pso} is the initial stress of tendon at time t_o; k is a constant depending on the steel type (equal to 1.5 and 0.667 for stress-relieved and low-relaxation steels, respectively); η_t is a dimensionless coefficient depending on the length of the period (t-t_o) and is given by

$$\begin{array}{lll} \frac{1}{16}\ln\left(\frac{t - t_o}{10} + 1\right) & for & 0 \le (t - t_o) \le 1000 \\ \left(\frac{t - t_o}{0.5x10^6}\right)^{0.2} & for & 1000 \prec (t - t_o) \le 0.5x10^6 \\ 1 & for & (t - t_o) \succ 0.5x10^6 \end{array} \qquad (15)$$

In the prestressed members the stressed steel commonly experiences a constantly reduction of its stress level with time due to the effects of creep and shrinkage of concrete. Thus, the actual relaxation, called *reduced relaxation*, is expected to be less than the intrinsic value. The reduced relaxation, $\Delta\overline{\sigma}_{pr}$, can be expressed as

$$\Delta\overline{\sigma}_{pr} = \chi_r\,\Delta\sigma_{pr} \qquad (16)$$

where the reduction coefficient,

$$\chi_r = \exp\left[\left(-6.7 + 5.3\frac{\sigma_{pso}}{f_{pu}}\right)\Omega\right] \qquad (17)$$

with

$$\Omega = \frac{\Delta\sigma_{ps} - \Delta\sigma_{pr}}{\sigma_{pso}} \qquad (18)$$

f_{pu} is the tensile strength of the tendon, and $\Delta\sigma_{ps}$ is the change in stress in tendon during a given period of time due to combined effects of creep, shrinkage and relaxation. This value does not known a priori as it depends on reduced relaxation, and therefore, iteration is necessary.

3 TIME-DEPENDENT FORMULATION FOR SEGMENTAL PRESTRESSED CONCRETE BRIDGES

A step-by-step scheme developed in [9] has been adopted here in this research to take into account the time-dependent effects in segmental prestressed concrete bridges. The time for which the bridge is analyzed is divided into intervals, and the stress increment for each interval is assumed to occur in the beginning of such interval. The bridge is modeled by an assemblage of linear non-prismatic elements. The conventional displacement-based element formulation has been utilized to calculate the incremental displacement and stress. Since the centroid of the reinforced concrete cross section changes its position with time due to varying its properties and cracking with time, the equations for calculating stress and strains have been written referred to an arbitrary reference point, O, which will be maintained constant through all steps of analysis. If a homogeneous elastic cross section is subjected to a normal force, N, and bending moment, M, at its arbitrary reference point O, the strain at any point of distance y from the point O can be expressed as

$$\varepsilon = \varepsilon_o + \kappa\, y \tag{19}$$

where ε_o is the strain at point O, and κ is the curvature, i.e., the slop of strain diagram. Stress distribution over the cross section can be calculated as $\sigma = E\,\varepsilon$ *(E is the Young's modulus).* The stress resultants, i.e., *N and M*, can be obtained by integrating the stress over the cross section as

$$\begin{Bmatrix} N \\ M \end{Bmatrix} = \begin{Bmatrix} \int \sigma\, dA \\ \int \sigma\, y\, dA \end{Bmatrix} = \begin{bmatrix} EA & ES_z \\ ES_z & EI_z \end{bmatrix} \begin{Bmatrix} \varepsilon_o \\ \kappa \end{Bmatrix} \tag{20}$$

Where A, S_z, and I_z are the cross section area, first and second moments of area about a transverse axis through point O, respectively. Alternatively, strain and curvature can be obtained in terms of normal force and bending moment as

$$\begin{Bmatrix} \varepsilon_o \\ \kappa \end{Bmatrix} = \frac{1}{E(AI_z - S_z^2)} \begin{bmatrix} I_z & -S_z \\ -S_z & A \end{bmatrix} \begin{Bmatrix} N \\ M \end{Bmatrix} \tag{21}$$

The instantaneous strain in a composite section made of concrete parts with different properties and several layers of prestressed and nonprestressed steels, due to increment on normal force ΔN and bending moment ΔM given by

$$\Delta N = \Delta N_{ext} - \sum P_j \tag{22a}$$

$$\Delta M = \Delta M_{ext} - \sum P_j \, y_{ps_j} \tag{22b}$$

can be obtained by Eq. (21) assuming that the composite section is replaced by a transformed section composed of area of concrete parts plus area of steels, each multiplied by its modulus of elasticity and divided by a reference value E_{ref}. ΔN_{ext} and ΔM_{ext}, in Eq.(22), represent the change in the internal forces due to external loads and the statically indeterminate effects of the initial prestressing applied at the instant considered; P_j is the prestressing force of post tension j^{th} tendon located at distance y_{psj} below point O, after deducting the losses due to friction and anchor set. The instantaneous stress distribution for each concrete part and steel layer can be determined. In general, the distribution of stress of each concrete part can be represented by a straight line, which defined by two parameters; (i) stress value at reference point O, and (ii) slope of stress distribution $d\sigma/dy$. If the total stress at the extreme tension fiber exceeds the concrete modulus of rupture, the section cracks. In this case, the area of concrete in the tension side of neutral axis is ignored, and the internal force is carried out by concrete in compression zone and reinforcement in tension zone.

The strain increment due to creep and shrinkage in an interval can be calculated from the stress applied in that interval and the proceeding ones. The creep of concrete are assumed to be linearly proportional to the applied stress; i.e., the stress increment Δf_c applied and sustain for a period of time produce instantaneous and creep strain equal to $\frac{\Delta f}{E_c}(1+\phi)$, where E_c is the modulus of elasticity of concrete which is a function of age of concrete and time of applied stress increment, and φ is a creep coefficient which is function of age concrete at loading and duration of sustain stress. If the time is divided into intervals during which the stress changes and creep and shrinkage occur freely, the change in concrete strain due to creep and shrinkage, during the i^{th} interval, is the difference of strain values calculated between time t_i and $t_{(i+1)}$; i.e.,

$$\begin{aligned}\Delta\varepsilon_c(t_{i+1},t_i)_{free} &= \frac{\Delta f_c\ (t_i)}{E_c\ (t_i)}\ \phi(t_{i+1}\ ,\ t_i) \\ &+ \sum_{j=1}^{i-1} \frac{\Delta f_c\ (t_j)}{E_c\ (t_j)}\left[\phi(t_{i+1}\ ,\ t_j) - \phi(t_i\ ,\ t_j)\right] + \Delta\varepsilon_s(t_{i+1},t_i)\end{aligned} \tag{23}$$

In the above, the first term is the creep strain caused by incremental stress $\Delta f_c(t_i)$ introduced at time t_i and ended at time $t_{(i+1)}$. The second term is the sum up of the effect of creep strains between time t_i and t_{i+1} due to stress introduced in proceeding time intervals. The third term is the free shrinkage between t_i and time t_{i+1}.

Once the two parameters, $[\Delta\varepsilon_o(t_{i+1},\ t_i),\ \Delta\kappa(t_{i+1},t_i)]_{free}$, defining the strain distribution over each concrete part are know, the time dependent changes in stress occurring in each concrete part and steel layer between t_i and t_{i+1} can be determined. The curvature $\Delta\kappa(t_{i+1},t_i)_{\text{free}}$ can be obtained by Eq.(23) by replacing σ by $d\sigma/dy$ and put $\Delta\varepsilon_s$ equal to zero. The hypothetical free strain in Eq. (23) can be prevented by introducing an artificial stress defined over concrete part j by stress by stress value at reference point O and slope as

$$\Delta\sigma_{o\,j}^{restraint} = -\left[\overline{E}_c(t_{i+1},t_i)\ \ \Delta\varepsilon_o(t_{i+1},t_i)_{free}\right]_j \quad ; \tag{24a}$$

$$\Delta(d\sigma_o/dy)_j^{restraint} = -\left[\overline{E}_c(t_{i+1},t_i)\ \ \Delta\kappa(t_{i+1},t_i)_{free}\right]_j \tag{24b}$$

where $\overline{E}_c(t_{i+1},t_i)_j$ is the age-adjusted modulus of elasticity of concrete part j [19]. The sum of stress resultants over concrete parts (ΔN^{cs}, ΔM^{cs}) from artificial stress can be determined from Eq. (20) as

$$\Delta N^{cs} = \sum_j \left(A_c\ \Delta\sigma_o^{restraint} + S_{zc}\left(\frac{d\sigma_o}{dy}\right)^{restraint}\right)_j \quad ; \tag{25a}$$

$$\Delta M^{cs} = \sum_j \left(S_{zc}\ \Delta\sigma_o^{restraint} + I_{zc}\left(\frac{d\sigma_o}{dy}\right)^{restraint}\right)_j \tag{25b}$$

Strain in concrete due to relaxation of prestressed steel can be artificially prevented by applying the summation of forces in the prestressed steel layers tensioned before or at time t_i *as*

$$\Delta N^{pr} = \sum_k \left(\Delta\overline{\sigma}_{pr}\ A_{ps}\right)_k \quad ; \quad \Delta M^{pr} = \sum_j \left(\Delta\overline{\sigma}_{pr}\ A_{ps}\,y_{ps}\right)_k \tag{26}$$

where A_{psk} and y_{psk} are the cross section area and y-coordinate of k^{th} prestressed steel layer.

Summing up the forces in Eq. (25, 26) gives ($\Delta N^{restraint}$, $\Delta M^{restraint}$), the total forces which would artificially prevent creep, shrinkage and relaxation. The artificial strain can be eliminated by applying forces with the same magnitude but in opposite directions on an age-adjusted transformed section composed of area of concrete in each part multiplied by $\overline{E}_c/E_{ref}$, plus area of reinforcement multiplied by $\overline{E}_s/E_{ref}$. Utilizing Eq. (21) with the properties of age-adjusted transformed section, such forces produce change in strain $\Delta\varepsilon(t_{i+1}, t_i)$ defined by its two parameters; i..e., (i) its value at reference point O, $\Delta\varepsilon_o(t_{i+1}, t_i)$, and (ii) the slop of the strain distribution, $\Delta\kappa(t_{i+1},t_i)$. Such strain can be multiplied by $\overline{E}_c$ of each concrete part gives the corresponding stress change. The total stress increment, then, can be calculated by the sum of this stress with the stress obtained in Eq. (24a), i.e.,

$$\Delta\sigma_c(t_{i+1}, t_i) = \Delta\sigma^{restraint} + \overline{E}_c \; \Delta\varepsilon_c(t_{i+1}, t_i) \tag{27}$$

Similarly, the change in stresses (between t_{i+1} and t_i) in prestressed and nonprestressed steels can be given by

$$\Delta\sigma_{ps}(t_{i+1}, t_i) = \Delta\overline{\sigma}_{pr} + E_{ps} \; \Delta\varepsilon_{ps}(t_{i+1}, t_i) \tag{28a}$$

$$\Delta\sigma_{ns}(t_{i+1}, t_i) = E_{ns} \; \Delta\varepsilon_{ns}(t_{i+1}, t_i) \tag{28b}$$

4 NONLINEAR OPTIMIZATION ALGORITHM

As alluded to the previously section, the optimization scheme in ESTMATOR formulates an objective optimization problem from information specified in data files, for both time dependent analysis response and two time independent analysis cases (simulated responses), and then solves it by using a sequential quadratic nonlinear programming technique [13-15]. To this end, we cast the optimal material parameters as the following non-linear mathematical programming problem:

> *find the n variables in $\underline{X}$ within prescribed upper and lower bounds, (i.e., $X_i^L \le X_i \le X_i^U$, i=1, 2, ... , n) to minimize the weighted function $\Im(\underline{X})$ under a set of inequality constraints n_g.*

In the above, $\underline{X}$ represents the independent, active, variables; e.g., see Eq. (31). The objective function can be expressed in terms of the following "error norms"

$$\Im(\underline{X}) = \frac{1}{2}\sum_{J=1}^{n_m}\left(1 - \frac{R_{E_j}}{R_{m_j}}\right)^2 \tag{29}$$

In the above, $\Im(\underline{X})$ is the objective function; n_m is the number of measurement stations along the specified bridge centerline; and R_{m_j} is the j$^{\underline{th}}$ stress/moment component obtained from the time dependent analysis, and R_{E_j} is the estimated stress/component obtained from the two contributions of the time independent analyses, i.e.,

$$R_{E_j} = \alpha \sum M_{o_j} + \beta M_{c_j} \tag{30}$$

where M_{o_j} is the stress/moment at the $j^{\underline{th}}$ station obtained from summation of all partial stresses/moments for each construction step using corresponding statical scheme; M_{c_j} is the corresponding one assuming all loads and prestress forces to be applied on the final statical system, and α and β are unknown variables in $\underline{X}$, i.e.,

$$\underline{X} = [\ \alpha\ ,\ \beta\ \ ]^T \tag{31}$$

Subject to the equality constraint,

$$g = \ \alpha + \ \beta = 1 \tag{32}$$

Utilizing a successive quadratic programming technique to solve the nonlinear programming problem simply amount to the following formal statements [Powell 1977]

$$\min_{\underset{\sim}{X} \in R^n} \Im(\underline{X}) \tag{33}$$

subject to

$$g_\ell(\underline{X}) = 0 \quad \mathit{for} \quad \ell = 1, 2, \ldots, n_E \tag{34a}$$

$$g_\ell(\underline{X}) \geq 0 \quad \mathit{for} \quad \ell = n_E, \ldots\ldots, n_g \tag{34b}$$

$$\underline{X}^L \ \leq \ \underline{X} \ \leq \ \underline{X}^U \tag{34c}$$

Such an optimization technique is based on iterative formulation and solution of quadratic programming sub-problems that can be obtained by using a quadratic approximation of the system's Lagrangian and linearizing of the constraints at the k<u>th</u> iteration as [Schittkowski 1983]

$$\min_{\underset{\sim}{d} \in R^n} \frac{1}{2} \underline{d}_k^T \ \underline{H}_k \ \underline{d}_k + \nabla \Im(\underline{X})^T \underline{d}_k \tag{35}$$

subject to

$$\nabla g_\ell(\underline{X})^T \ \underline{d}_k + g_\ell(\underline{X}) \ \geq \ 0 \quad , \ \ell = 1, 2, \ldots\ldots, n_g \tag{36a}$$

$$\underline{X}^L - \underline{X}_k \leq \underline{d}_k \leq \ \underline{X}^U - \underline{X}_k \tag{36b}$$

where $\underline{d}_k$ is the solution of the sub-problem; $\underline{H}_k$ is the positive definite approximation of the Hessian matrix; $\underline{X}_k$ is the variables at the k<u>th</u> iteration; $\nabla \Im(\underline{X})$ is the gradient of the objective function;

$$\frac{\partial \Im(\underline{X})}{\partial X_i} = \sum_{j=1}^{n_m} \left(1 - \frac{R_{E_j}}{R^2{}_{m_j}} \right) \frac{\partial R_{E_j}}{\partial X_i} \tag{37}$$

and $\nabla g_\ell(\underline{X})$ is the gradient of the ℓ <u>th</u> active constraint.

A line search scheme is then used to fined a new variable $\underline{X}_{k+1}$,

$$\underline{X}_{k+1} = \underline{X}_k + \eta \, \underline{d}_k \qquad \eta \in (0,1], \tag{38}$$

such that the objective function $\Im(\underline{X}_{k+1})$ has a lower value at the new state variable $\underline{X}_{k+1}$.

Once the optimum variables are determined by ESTMATOR, the quality of the model's correlation with the results obtained by time dependent analysis can be assessed. This is simply done by using any plotting capability to graphically show how well the model's prediction of the time dependent behavior. At this point, the user has to judge whether the parameters determined by ESTMATOR are acceptable.

5 NUMERICAL SIMULATIONS

The primary objective of this section is of two-fold: (i) to obtain the time dependent serviceability analysis of two segmental prestressed concrete bridges over the Nile River, namely Warrak Bridge, and Talkha Bridge; and (ii) to assess the accuracy of the developed integrated algorithms through software ESTMATOR to obtain optimum parameters simulating the time-dependent results from two different cases of time independent analyses. The ESTMATOR casts the optimum parameters as a minimum-error nonlinear optimization problem with constraints and solves it with the sequential quadratic nonlinear programming technique. With regard to item (i) above, the bridge superstructure is modeled as an assemblage of 2-node one-dimensional linear beam elements. Each element represents the cast segment of the bridge. The beam element is of layer-type, that is, the cross section of the element is divided into several layers; each layer may consist of concrete, reinforcing bars and prestressing tendons. Each node of the element consists of two translational degrees of freedom and one rotational degree of freedom. The strains of each layer of the element consist of centroidal axial strain, and curvature. The corresponding generalized forces, i.e., axial force and bending moment, are obtained from integrating corresponding layer stresses over the entire cross section. In the formulation of stiffness matrix, the Bernoulli-Euler assumption of "plane section remains plane" is adopted. Since the piers are integrally cast with the superstructure, they are modeled as beam elements to account for the moment transfer between superstructure and piers.

5.1 A case study: Talkha Bridge

Talkha Bridge is being constructed across Demietta branch of the Nile River to connect the north and south parts of the Nile at Talkha city which is located in the Delta of Egypt. The bridge consists of four lanes; two lanes for each traffic direction. The superstructure consists of two parallel identical box girders which are completely separated along the longitudinal direction of the bridge. The cross sections of the box girder at mid-span and at piers are shown in *Fig. 1*. The width of the top slab is 10.5 m.; while width of the bottom slab varies from 4.90 m at the mid-span to 3.80 m. at the piers. The height of the cross section varies parabolicly to be 3.0 m at mid-span and 5.50 m at the piers. The final bridge structure consists of three continuous spans; i.e, two side spans and one main (navigation) spans as shown in Fig. 2. The side span is 65.0 m long and the main span is 100.0 m long. The bridge is supported by slide bearings on edge piers and cast integrally with intermediate piers. The longitudinal prestressing layout is shown in *Fig. 2*. Each prestressing tendon consists of 12 strands. The strand is 15.2-mm diameter 7-wire low relaxation type. The number of top tendons is 38 around each pier; while the number of bottom continuity tendons is 18 in main span and 14 in each side span. The tendons are initially stressed to 75% of the ultimate tensile strength (UTS).

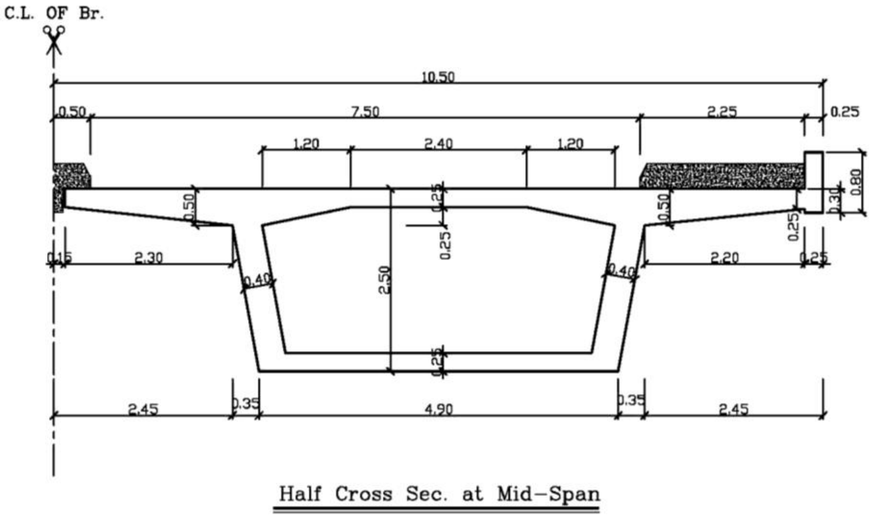

Figure 1. Cross-sections of Talkha bridge

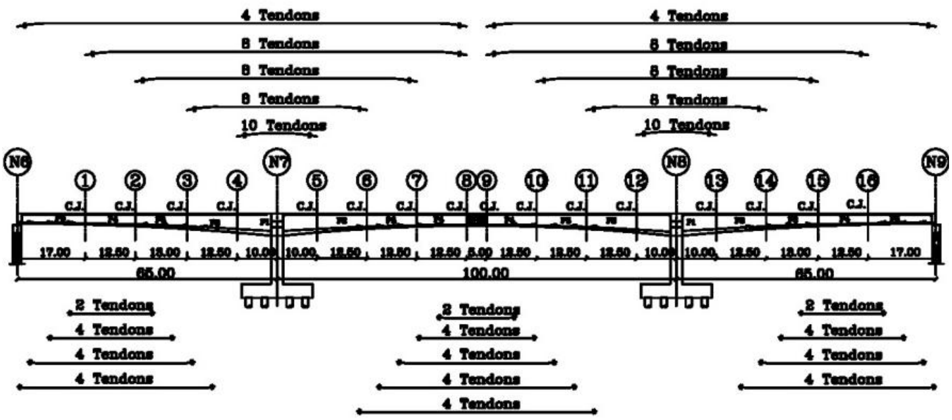

Figure 2. Longitudinal profile of the prestressing tendons of Talkha bridge

The bridge is incrementally constructed as balanced cantilever from piers N7, and N8 such that two parts with equal weight can be constructed at the same time around each pier. Piers at axes N7 and N8 consist of 4 cast-in-place segments for each pier. Each segment is cast utilizing conventional formwork in 30 days, while the construction of each pier takes 90 days. The construction of first segment around N8 starts after constructing the first two segments around N7. After constructed each segment, sufficient tendons are tensioned in top slab to carry its own weight, then the formwork is removed. On the two sides of the river, the 17.50 m long side span is cast on temporary scaffolding and connected with the double cantilevers located at axes N7 and N8. After the side span hardens, 6 bottom tendons are tensioned in each side span. The construction of each side span takes 30 days. The tips of the cantilevers in the navigation span are, then, connected by a 5.0 m closure segment. After the closure segment hardens, 18 bottom tendons are prestressed in the navigation span along with 8 bottom tendons in each of the side span. The construction of the entire bridge takes 315 days. After bottom tendons are prestressed, the structure achieves the continuous form. Any load applied afterwards, for example, the superimposed load including asphaltic wearing surface and safety barrier, traffic loads and other live loads will act on the continuous structure.

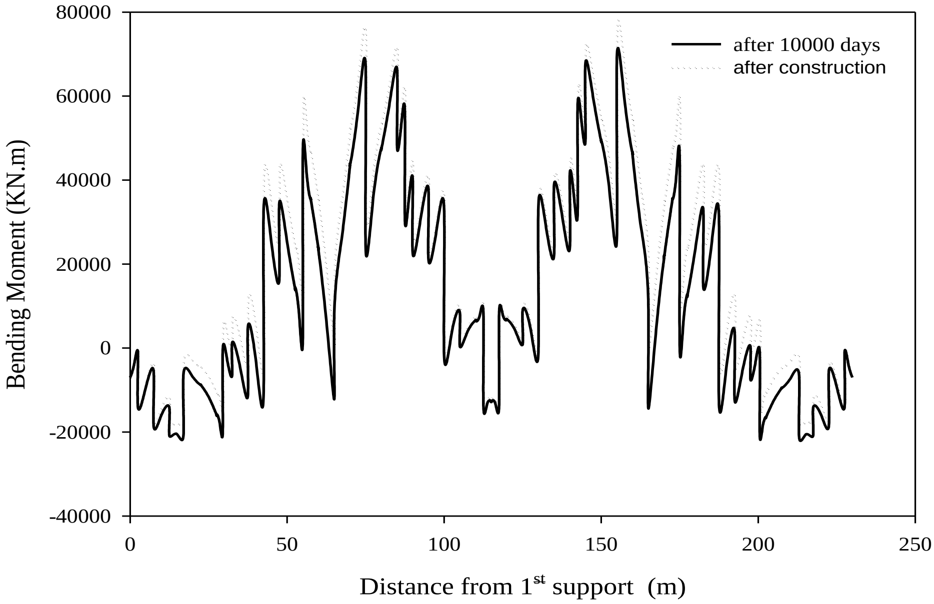

Figure 3. Bending moments due to own weight and prestressing

The bending moments in the box girder due to its own weight obtained utilizing the time dependent effects for two time observations; i.e., (i) after completing the construction, (ii) after 10000 days are shown in *Fig. 3*. These moments are obtained by integrating the stress over the cross section and include the effect of prestressing and non-prestressing reinforcement. The time dependent moments after 10000 days exhibited little redistribution compared to those obtained after completing the construction. The stresses in the concrete sections, however, do redistribute. This is mainly due to the loss in prestressing force in tendons. The negative moments in the box girder near the piers increase over time demonstrating that the increase in the negative moment due to loss of prestressing force is greater than the decrease in negative moment due to dead load moment redistribution. At the center of main span, the negative moment is slightly increased over time. The prestressing force along the entire bridge is shown in *Fig. 4* for two observation times, (i) just after construction, (ii) after 10000 days. The percentage losses of the force in the prestressing tendons after completing the construction and after 10000 days compared to the corresponding force after transfer about 7% and 17% at sections near piers, respectively, and about 4% and 17% at center of main span. The compression forces in normal reinforcements are increased over time as shown in *Fig. 4*. After 10000 days, such compression forces are about 16% of the prestressing force at section near pier, and 29% at section at center of main span. Stress redistribution in top and bottom fibers of the concrete at critical sections starting from time at completing construction to time at 10000 days are shown in *Fig. 5*.

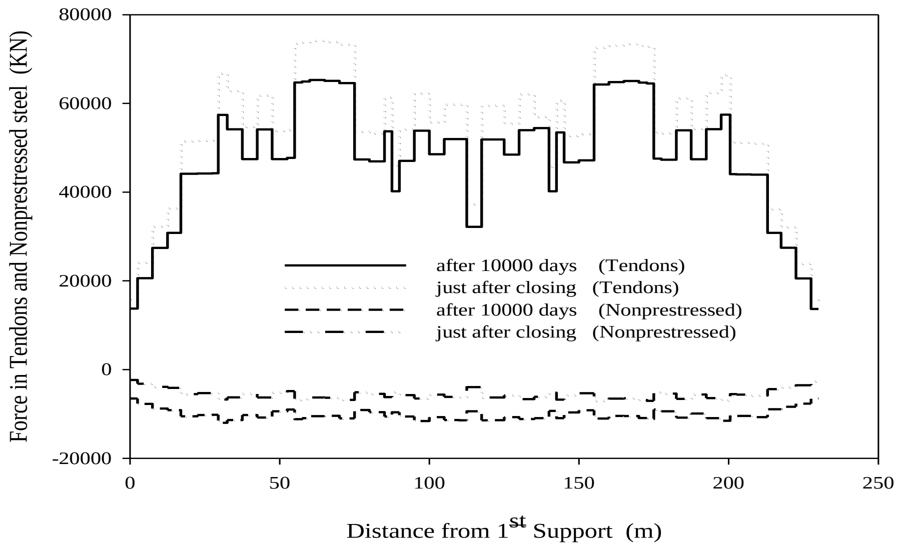

Figure 4. Forces in prestress and nonprestress steels

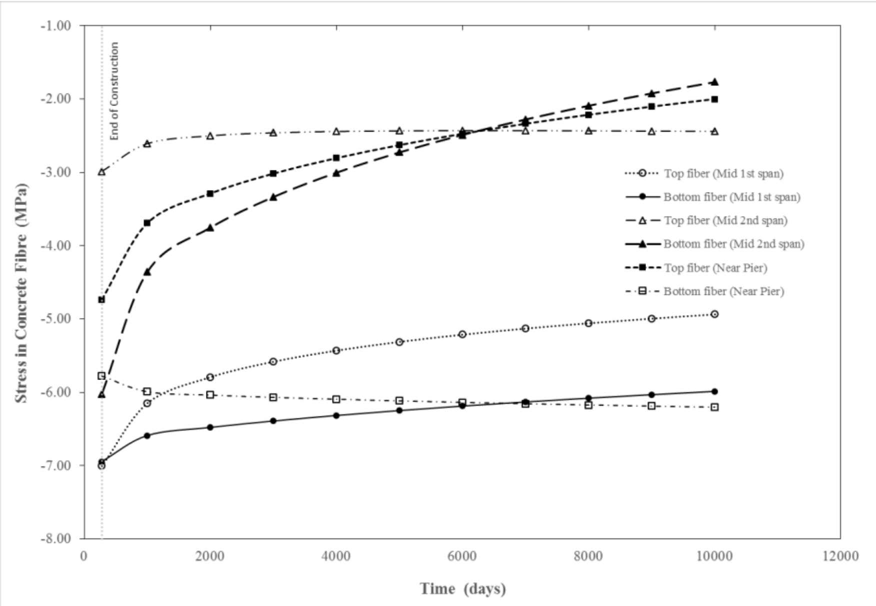

Figure 5. Stress distributions over time at critical sections of Talkha Bridge

It is worthy noted that a small change in moment causes a significant change in stress due to the reduction of prestressing force. As an evidence from this figure, the stresses in the top and bottom fibers of all critical sections decrease with time, except the stress in bottom fiber of the section at pier. In such section, the stress slightly increases with time which reveals the increase in negative moment at this section.

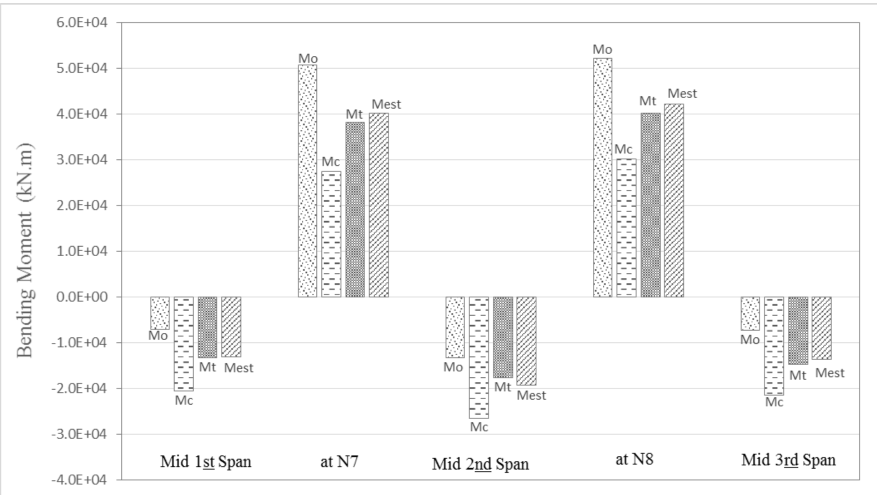

Figure 6. Estimated moments with ESTMATOR at critical sections

The optimization methodology developed in ESTMATOR has been utilized to simulate the time dependent moments obtained after 10000 days for Talkha Bridge from the two contributions of the time independent analyses obtained by: (i) adding all partial moments for each construction step using corresponding statical system; (ii) assuming all loads and prestressing forces to be applied on the final statical system. We start the optimization exercise with a set of initial values for the parameters a and β equal to 0.5. The lower and upper bounds are kept between 0.0 and 1.0, respectively. The optimum values for the two parameters identified with ESTMATOR are 0.545 and 0.455, respectively. Upon comparing the estimated moments at the critical sections obtained with optimum values with those obtained with time dependent effects, it is evident from *Fig. 6* that ESTMATOR accurately matches the moments provided by the time dependent analysis.

5.2 Case study of EL-Warrak Bridge

Warrak Bridge is one of the longest segmental prestressed concrete bridges over the Nile River in Egypt. Such bridge is 380 m in length, with maximum span length of 120 m. The bridge consists of four-spans with four-cell hunched box cross section. It has eight lanes; i.e., four lanes for each traffic direction. Each double cell is completely separated in the longitudinal direction of the bridge. The double-cell box has slanted webs and two side cantilevers providing a roadway 22.65 m. wide, as shown in *Fig 7*. The hunched box girder is cantilevered from the piers using cast-in-place segments, and is later made continuous with a short, conventionally erected, cast-in-place girder near the abutments and with the adjoining cantilevered girder at mid-span. Each cantilever segment is post tensioned to the previous segments with several ‘’cantilever’’ tendons, and after the closures at the abutments and at mid-span the entire bridge is prestressed with several additional ‘’continuity’’ tendons in zones with high positive moments. This is a common construction sequence and prestressing scheme for bridges of this type. The details of the design, the design criteria and the construction sequence are discussed below.

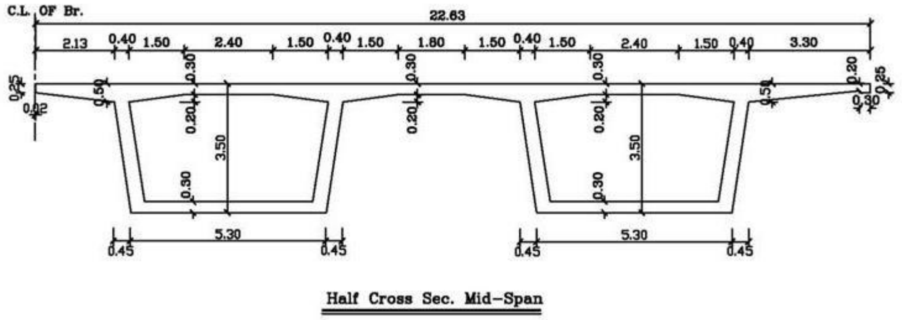

Figure 7. Cross-sections of El-Warrak bridge

The span arrangement consists of two 120 meter center spans and two 70 meter side spans as shown in *Fig. 8*. The girder depth varies over the length following second degree parabola from maximum of 6 m. over the piers to minimum of 3.50 m. at the middle of the main spans. The thickness of the bottom slab varies also parabolically from a maximum of 1.20 m. at the piers to a minimum of 0.30 m. at the middle of main span. The bridge is built using the cantilever method. Three double cantilever parts can be constructed independently, i.e., around O, P and Q axes. Each double cantilever can be constructed in segments starting from the pier towards the center spans, i.e., one segment from the right end followed by another one from the left end. Each segment is 5.0 m. long except three segments of length 2.5 m. (i.e, one near each pier) to keep the unbalanced length between the two arms of the cantilevers during construction equal to 2.5 m. Two travelers, one at each tip of the two cantilevers, are utilized to erect segments. After erection of each segment, it is post tensioned to the previous segment (i.e., on the other end of the double cantilever) with ‘’cantilever’’ tendons located in the top slab of the cross section. Each cantilever tendon consists of 12, 0.6 inch (15.7 mm.) diameter strands and is stressed from one end.

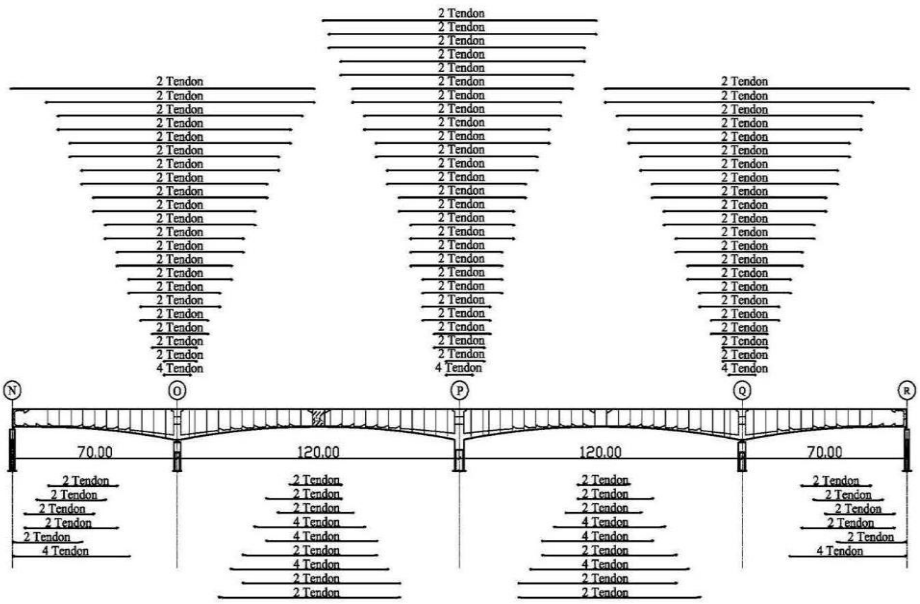

Figure 8. Longitudidal profile of prestressing tendons of El-Warrak Bridge

The bridge is incrementally constructed as balanced cantilever from piers O, P, and Q. Piers at axes O and Q consist of 21 cast-in-place segments for each pier, while 20 segments are constructed around axis P. Each segment is cast utilizing conventional formwork in 7 days, while the construction of each pier takes 90 days in additional to 14 days for the stump. The construction of stump at axis Q starts after constructing the first five segments around axis O, while the stump at axis P starts after constructing the entire segments around axis O. On the two sides of the river, the 17.50 m long side span is cast on temporary scaffolding and connected with the double cantilevers located at axes O and Q. After the side span hardens, 8 bottom tendons are tensioned in each side span. The construction of each side span takes 15 days. The tips of the cantilevers in the navigation spans are, then, connected by a 5.0 m closure segments. After the two closure segments harden, 28 bottom tendons are prestressed in each of the navigation span along with 6 bottom tendons in each of the side span. The construction of the entire bridge takes 447 days. After bottom tendons are prestressed, the structure achieves the continuous form. Any load applied afterwards, for example, the superimposed load including asphaltic wearing surface and safety barrier, traffic loads and other live loads will act on the continuous structure.

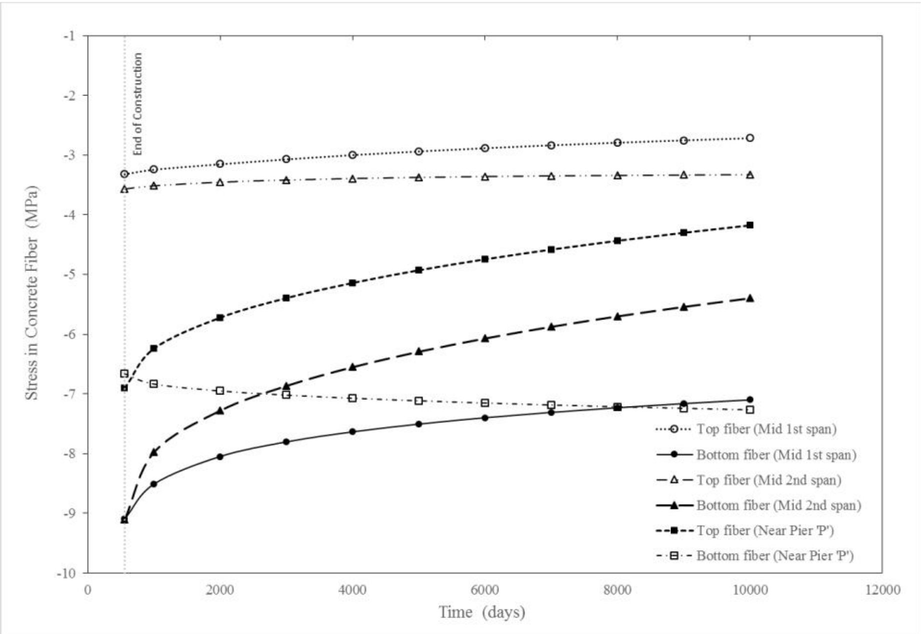

Figure 9. Stress distributions over time at critical sections of El-Warrak Bridge

The percentage losses of the force in the prestressing tendons after completing the construction and after 10000 days compared to the corresponding force after transfer are about 11% and 21% at sections near piers, respectively, and about 5.5% and 19.5% at center of main span. Stress redistribution in top and bottom fibers of the concrete at critical sections starting from time at completing construction to time at 10000 days are shown in *Fig. 9*. It is worthy noted that a small change in moment causes a significant change in stress due to the reduction of prestressing force. As an evidence from this figure, the stresses in the top and bottom fibers of all critical sections decrease with time, except the stress in bottom fiber of the section at pier. In such section, the stress slightly increases with time which reveals the increase in negative moment at this section.

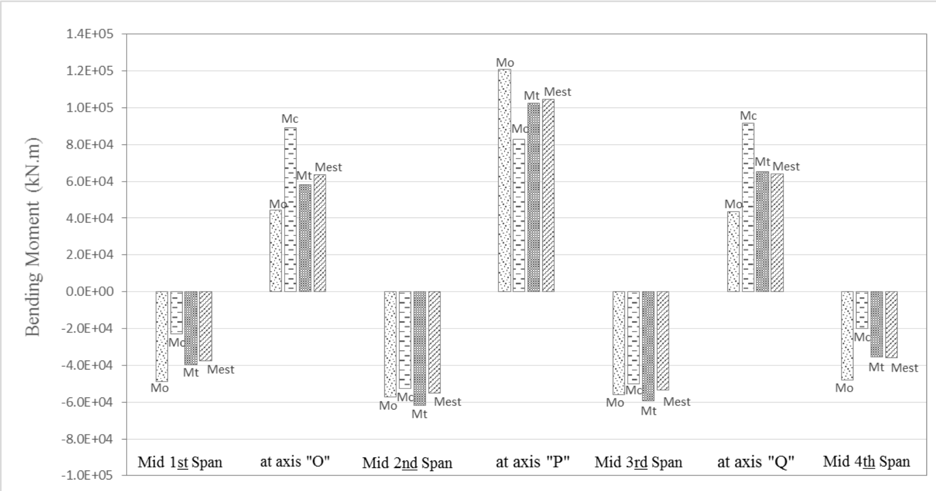

Figure 10. Estimated moments with ESTMATOR at critical sections of El-Warrak Bridge

The optimization methodology developed in ESTMATOR has been utilized to simulate the time dependent moments obtained after 10000 days for such Bridge from the two contributions of the time independent analyses obtained by: (i) adding all partial moments for each construction step using corresponding statical system; (ii) assuming all loads and prestressing forces to be applied on the final statical system. We start the optimization exercise with a set of initial values for the parameters a and β equal to 0.5. The lower and upper bounds are kept between 0.0 and 1.0, respectively. The optimum values for the two parameters identified with ESTMATOR are 0.572 and 0.428, respectively. Upon comparing the estimated moments at the critical sections obtained with optimum values with those obtained with time dependent effects, it is evident from *Fig. 10* that ESTMATOR accurately matches the moments provided by the time dependent analysis.

5.3 Effect of construction time schedule on moment redistribution

This study presents the effect of the construction time schedule of the segmental bridges on the moment redistribution. Such study made over real bridges, i.e. El-Warrak bridge and Talkha bridge. Using the CPF computer program, analyses of these bridges are considered for different time of construction. These bridges have been analyzed in sections 5.2 and 5.3 with the real construction time schedule; i.e., called, "normal case". Here, the same two bridges are analyzed with two other construction time schedules; i.e., one is faster and the other is slower than the real construction (normal case). These two cases are called "fast case" and "slow case", respectively. In fast case, constructions of segments around all piers start and finish simultaneously. The time for constructing Talkha and El-Warrak bridges using the fast schedule is 255, and 304 days, respectively. On the other hand, in slow case, segments of double cantilever around each pier constructed sequentially. The time for constructing Talkha and El-Warrak bridges with slow schedule is 420 and 875 days, respectively.

The optimization methodology in ESTAMATOR has been utilized to simulate the time dependent moments obtained after 10000 days for these bridges for the other two cases; i.e. fast and slow cases. The two contributions of the time independent analyses obtained by: (i) superposition all partial moments for each construction step using the corresponding statical system; (ii) assuming all loads and prestressing forces to be applied on the final statical system. We start the optimization exercise with a set of initial values for the parameters α and β equal to 0.5. The lower and upper bounds are kept between 0.0 and 1.0, respectively. The optimum values for the two parameters identified with ESTMATOR as shown in Table 1.

Table 1. Values of parameters α and β for different time schedules

	parameters α and β	construction time schedule		
		fast	Normal	slow
Talkha Bridge	α	0.390	0.545	0.632
	β	0.610	0.455	0.368
El-Warrak Bridge	α	0.378	0.572	0.749
	β	0.622	0.428	0.251

The estimated moments at the critical sections obtained with optimum values are in good agreement with those obtained with time dependent effects; i.e., ESTMATOR accurately matches the moments provided by the time dependent analysis. As shown from this table, the parameters α and β range between two limits; i.e., 0.38 and 0.62 for fast time schedule of construction, and 0.75 and 0.25 for slow time schedule of construction.

6 CONCLUSIONS

Details of several algorithmic developments have been presented as parts of an overall strategy to estimate the parameters needed to predict the time dependent effects of segmental prestressed concrete bridges from the conventional analyses in which the time dependent effects have been ignored. These algorithms were subsequently incorporated into optimization software (ESTMATOR). In this, a general time-stepping algorithm for stress-update is developed for concrete, prestressed and non-prestressed steels. This includes time dependent effects due to creep and shrinkage of concrete utilizing Eurocode, relaxation of prestress steel, losses due to friction and anchor setting of prestressed tendons; and sequence of construction and change of geometry and support conditions (if any). The optimization module in ESTMATOR is used to cast the estimation of the parameters as a minimum-error, objective, nonlinear optimization problem, which is subsequently solved using the sequential quadratic programming technique. Suitable error functions were utilized as the basis for the last phase of optimization.

Regarding applications, two segmental prestressed concrete bridges over the Nile river have been investigated. The first is called Talkha Bridge in Delta, while the other is called Warrak Bridge in Cairo, Egypt. The results obtained have clearly demonstrated the great potential, effectiveness, as well as practical utility of the proposed methodology. In particular, a number of pertinent remarks are summarized below:

(i) The capability of the develop scheme can handle a realistic, large scale, multi-span prestressed concrete box girder built using the cantilever method, utilizing cast in place segments, traveling formwork, conventionally erected girder segments near the abutments, and temporary supports.

(ii) Prediction of stresses and deformations in segmentally erected prestressed concrete bridges can be considerably in error if the effects of creep, shrinkage, and relaxation are ignored.

(iii) The overall static equilibrium of the girder slightly changes over time in comparison with the internal stresses in the girder. Changes in moment due to creep and its associated moment redistribution are nearly balanced by changes in moment due to losses in prestressing force.

(iv) ESTMATOR predicted the time dependent moments at different sections of bridges from two time independent analysis models; i.e., the first one following the construction sequence by superposition all partial moments for each construction step using its corresponding statical system; while the second assuming all loads and prestressing forces to be applied on the final statical system. Several conclusions can be summarized as:

   a. Estimated parameters to simulate the time dependent analysis are sensitive to the time schedule of construction.
   b. For normal time schedule of construction, the recommended

parameters are 0.55 and 0.45 for α and β, respectively.

c. The parameters α and β ranged between two limits; i.e., 0.38 and 0.62 for fast time schedule of construction, and 0.75 and 0.25 for slow time schedule of construction.

REFERENCES

[1] Ketchum, M. A., "Redistribution of stresses in segmentally erected prestressed concrete bridges", UCB/SESM-86/07. Department of Civil Engineering, University of California, Berkeley, 1986.

[2] Kwak, H. G., and Seo, Y.J.,"Long-term behavior of composite girder bridges. Comput Struct 2000;74:583–99.

[3] Bishara, A. G. and Papakonstantinou, N.G., "Analysis of cast-in-place concrete segmental cantilever bridges", J Struct Eng, ASCE 1990;116(5):1247–68.

[4] Chiu, H.I., Chern, J.C., and Chang, K.C., "Long-term deflection control in cantilever prestressed concrete bridges I: Control method", J Eng Mech, ASCE 1996;12(6):489–94.

[5] Trost, H., and Wolff, H.J. Zur wirklichkeitsnahen ermittlung der beanspruchungen in abschnittswiese hergestellten spannbetonragwerken. Structural Engineering Documents ie, Concrete Box-Girder Bridge, IABSE, 1982.

[6] Cruz, PJS, Mari, A.R., and Roca, P., "Nonlinear time-dependent analysis of segmentally constructed structures", J Struct Eng, ASCE 1998;124(3):278–88.

[7] Barker, J.M., Post-tensioned box girder manual, USA: Post-Tensioning Institute, 1997.

[8] Kwak, H. G., and Seo, Y.J., "Determination of design moments in bridges constructed by balanced cantilever method," Engineering Structures, 24 (2002) 639–648

[9] Tadros, M.K., Ghali, A., and Dilger, W.H., "Long Term Stresses and Deformations of Segmental Bridges," Prestresses Concrete Institute, PCI Journal, Vol. 24, No. 4, 1979, 66-78.

[10] EC 2. Eurocode 2: Design of concrete structures_Part 1-1: General rules and rules for buildings. Brussels: EN 1992-1-1, CEN; 2004.

[11] MC 90, CEB-FIP model code 1990. 6th ed. London: Thomas Telford; 1993

[12] Powell, M.J.D., “A Fast Algorithm for Nonlinearly Constrained Optimization Calculations”, in Numerical Analysis proceedings, Dundee 1977, Lecture notes in Mathematics (edited by G.A. Waston) 630, Springer-Verlag, Berlin, Germany, 144-157.

[13] Schittkowski, K. “Nonlinear Programming Code”, Lecture notes in Eronotics and Mathematical Systems 183, Springer-Verlag, Berlin, Germany, 1980.

[14] Schittkowski, K., “On the Convergence of a Sequential Quadratic Programming Method with an Automated Lagrangian Line Search Function”, Mathematik Operations forschung and Statistik, Serie Optimization 14, pp. 197-216, 1983.

[15] Schittkowski, K., “NLPQL: A Fortran Subroutine Solving Constrained Nonlinear Programming Problems”, in Annals of Operations Research, Clyde L. Monma, (ed.) 5, pp. 485-500, 1986.

[16] Leunberger, D.G., Linear and Non linear Programming, 2nd Edition, Addison – Wesley, Reading, 1984.

[17] Ghali, A., and Trevino, J., "Relaxation of Steel in Prestressed Concrete," Prestresses Concrete Institute, PCI Journal, Vol. 30, No. 5, 1985, 82-94.

[18] Federation Internationale de la Precontrainte (FIP), Report on Prestressing Steel, Part 1 – Types and Properties. FIP/5/3/, Cement and Concrete Association, England, August 1976.

[19] Bazant, Z. P., "Prediction of Concrete Creep Effects Using Age-Adjusted Effective Modulus Method", Journal of the American Concrete Institute, ACI Proceedings, Vol. 69, No. 4, April 1972, 212-217.